



# Non-homogeneous approximation for the kurtosis evolution of shoaling rogue waves

Saulo Mendes <sup>1,2,\*</sup> and Jérôme Kasparian <sup>1,2,†</sup>

<sup>1</sup>*Group of Applied Physics, University of Geneva, 1205 Geneva, Switzerland*

<sup>2</sup>*Institute for Environmental Sciences, University of Geneva, 1205 Geneva, Switzerland*

Bathymetric changes have been experimentally shown to affect the occurrence of rogue waves. In view of the central role played by the excess kurtosis of the surface elevation in estimating rare event probabilities, we translate the recently determined evolution of the rogue wave probability over a shoal into that of the kurtosis. We provide an effective theory that connects the non-homogeneous correction to the spectral analysis and the evolution of excess kurtosis over the shoal, as well as the kurtosis upper bound. In intermediate water depth the vertical asymmetry between crests and troughs is virtually constant throughout the shoal for a given wave steepness and bandwidth, thus not affecting the exceedance probability. Conversely, a sharp increase in steepness increases the asymmetry for waves in intermediate depth. Thus, both the tail of the exceedance probability and excess kurtosis grow.

## I. INTRODUCTION

Ocean wave statistics is at the crossroads of ocean engineering and physical oceanography. Ocean engineers are commonly concerned with both short-term and long-term waves statistics [1], while the mechanisms responsible for the formation of extreme waves is the focus in physical oceanography [2]. The unexpected observation of the so-called rogue waves (also known as freak waves) over the past decades [3] reignited the cross-disciplinary interest in wave statistics. These waves seemingly “appear from nowhere” [4], and are by statistical definition at least twice taller than the significant wave height. From an engineering perspective, the performance of theoretical probability models at the tail of the distribution measures their practical success.

Applying the signal processing methods of Rice [5], the bulk of surface gravity waves were demonstrated to follow a Rayleigh distribution of heights [6]. Nevertheless, the Rayleigh distribution is unsuited to capture the tail of the distribution in real ocean conditions [7, 8]. On the other hand, nonlinear theories and their associated probability distributions are inaccurate in a wide range of real ocean conditions [9, 10]. These difficulties were realized early on, such that the Longuet-Higgins [11] handling of a non-Gaussian distribution of the sea surface elevation through a factorization of skewness and excess kurtosis from the normal distribution has been widely favoured. Moreover, approaches to compute surface elevation, crest and wave height distributions require methodologies that are often computationally burdensome [12]. Naturally, the excess kurtosis became the centre of wave statistics in an attempt to transfer the problem from the probability distribution to the cumulant expansion [13, 14]. The complexity of water wave solutions led to the use of excess kurtosis as an alternative to the evaluation of statistical distributions [15, 16].

To connect both frameworks, we provide an effective theory based on energy density redistribution [17] to describe the evolution of kurtosis of wave trains travelling over a shoal. Moreover, as a key element for the amplification of rogue wave probability due to a shoal, we obtain an approximation for the vertical asymmetry between crests and troughs as a function of water depth, bandwidth and steepness. Rogue waves travelling past a shoal are amplified with little regard for vertical asymmetry variations when  $k_p h > 0.5$ , unless either the spectrum is significantly broad-banded ( $\nu > 0.5$ ) or the steepness is large ( $\varepsilon > 1/10$ ). Accordingly, these formulae lead to an upper bound for the excess kurtosis, of paramount importance for naval design purposes.

## II. THEORETICAL CONSIDERATIONS

We review the main ideas of the theory of non-homogeneous analysis of water waves travelling over a shoal [17]. Given a velocity potential  $\Phi(x, z, t)$  and surface elevation  $\zeta(x, t)$ , the average energy density evolving over a shoal described by  $h(x) = h_0 + x\nabla h$  with finite constant slope  $1/20 \leq |\nabla h| = |h_f - h_0|/L < 1$  (see figure 1) is expressed as:

$$\mathcal{E} = \frac{1}{2\lambda} \int_0^\lambda \left\{ \left[ \zeta(x, t) + h(x) \right]^2 - h^2(x) + \frac{1}{g} \int_{-h(x)}^\zeta \left[ \left( \frac{\partial \Phi}{\partial x} \right)^2 + \left( \frac{\partial \Phi}{\partial z} \right)^2 \right] dz \right\} dx, \quad (1)$$

with zero-crossing wavelength  $\lambda$  and gravitational acceleration  $g$ . An inhomogeneous elevation  $\zeta(x, t)$  perturbs the energy partition and redistributes the wave energy density, thus modifying the probability density of water waves. The spectral analysis consistent with an inhomogeneous energy defines a correction ( $\langle \cdot \rangle_t$  stands for temporal average):

$$\Gamma(x) \approx \frac{\langle \zeta^2(x, t) \rangle_t(x)}{\mathcal{E}(x)}, \quad (2)$$

\* saulo.dasilvamendes@unige.ch

† jerome.kasparian@unige.ch

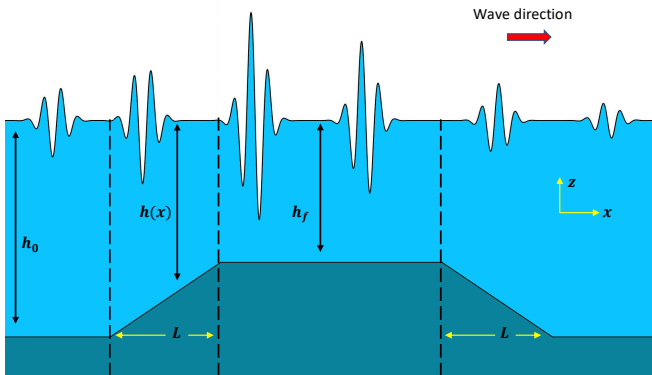


FIG. 1: Portraying of the extreme wave amplification due to a bar [17]. The water column depth evolves as  $h(x) = h_0 + x\nabla h$  with slope  $\nabla h = (h_f - h_0)/L$ . Dashed vertical lines delineate shoaling and de-shoaling regions as in figure 2.

dependent on the steepness  $\varepsilon = H_s/\lambda$  and depth  $k_p h$ , with  $H_s$  being the significant wave height (the average among the 1/3 largest waves). The inhomogeneity of both  $\mathcal{E}(x)$  and  $\langle \zeta^2 \rangle_t(x)$  redistributes energy and transforms the pre-shoal Rayleigh exceedance probability into:

$$\mathbb{P}_{\alpha, \Gamma}(H > \alpha H_s) = \int_{\alpha}^{+\infty} \frac{4\alpha_0}{\Gamma} e^{-2\alpha_0^2/\Gamma} d\alpha_0 = e^{-2\alpha^2/\Gamma} (3)$$

For linear waves ( $\varepsilon \ll 1/100$ )  $\Gamma = 1$  and we recover the case of a Gaussian sea. The evolution of the exceedance probability  $\mathbb{P}(H > \alpha H_s)$  in eq. (3) can be generalized to any arbitrary incoming statistics [17]:

$$\ln \left( \frac{\mathbb{P}_{\alpha, \Gamma \mathfrak{S}}}{\mathbb{P}_{\alpha}} \right) \approx 2\alpha^2 \left( 1 - \frac{1}{\mathfrak{S}^2(\alpha)\Gamma \mathfrak{S}} \right) \quad , \quad (4)$$

with the mean vertical asymmetry between crests and troughs (twice the mean ratio of crest to wave heights) of rogue waves expressed as [18],

$$\mathfrak{S}(\alpha = 2) \approx \frac{2\eta_s}{1 + \eta_s} \left( 1 + \frac{\eta_s}{6} \right) \quad , \quad \eta_s \approx 1 + \mu_3 \quad , \quad (5)$$

obeying  $1 \leq \mathfrak{S} \leq 2$  for all  $\alpha$  and with  $\eta_s$  measuring the ratio between mean crests and mean troughs, empirically found to depend on the skewness [18]. When the water depth decreases waves become steeper while the super-harmonic contribution has an increasing share of the wave envelope. The combination of these two effects redistributes the exceedance probability by causing the rise in  $\langle \zeta^2 \rangle$  to exceed the growth of  $\mathcal{E}$ . Such uneven growth explains why a shoal in intermediate water amplifies rogue wave occurrence as compared to deep water [19, 20] while it reduces this occurrence in shallow water [21, 22]. The linear term in  $\zeta(x, t)$  has the leading order in deep water and  $\Gamma - 1 \lesssim 10^{-2}$  is small. Conversely, in intermediate water the sub-harmonic creates significant disturbances in the energy density increasing  $\Gamma - 1$

up to  $10^{-1}$ , whereas in shallow water the sub-harmonic diverges and  $\Gamma - 1 \lesssim 10^{-3}$  becomes small again, reading even smaller values than in deep water.

### III. KURTOSIS EVOLUTION OVER A SHOAL

The probability evolution of eq. (3) depends solely on  $\Gamma$ . However, any deviation from a Gaussian distribution may be described by a cumulant expansion [11] which at leading order is expressed as a function of the excess kurtosis  $\mu_4$ . For the case of an inhomogeneous wave field due to a shoal, there is an excess in kurtosis due to the energy partition. The probability ratio relative to the Rayleigh distribution (implying a pre-shoal  $\mu_4 = 0$ ) is computed through the transformation of variables from the wave envelope in Mori and Yasuda [23] into normalized heights, to leading order in  $\mu_4$  computed in section 6.2.3 of Mendes [24]:

$$\frac{\mathbb{P}_{\alpha, \mu_4}}{\mathbb{P}_{\alpha}} \approx 1 + \mu_4 \frac{\alpha^2}{2} (\alpha^2 - 1) + \mu_3^2 \frac{5\alpha^2}{18} (2\alpha^4 - 6\alpha^2 - 3) (6)$$

For all  $\alpha \geq 1$ . Taking into account the theoretical relation  $\mu_4 \approx 16\mu_3^2/9$  between kurtosis and skewness confirmed by wave shoaling experiments [25], we rewrite eq. (6):

$$\frac{\mathbb{P}_{\alpha, \mu_4}}{\mathbb{P}_{\alpha}} \approx 1 + \mu_4 \cdot \frac{\alpha^2}{32} (10\alpha^4 - 14\alpha^2 - 31) \quad , \quad \forall \alpha \gtrsim 2 \quad (7)$$

The kurtosis measures tailness and it affects the exceedance probability for  $\alpha \gtrsim 1.5$ . Eqs. (4) and (7) describe the physical effect of energy redistribution and the associated deviation from a Gaussian sea. They can be matched, yielding a kurtosis  $\mu_4(\Gamma, \alpha)$ . Therefore, we evaluate both equations at  $\alpha = 2$  as it stays within  $\pm 20\%$  over the range of validity and stability of eq. (7) ( $2 \lesssim \alpha \lesssim 3$ ), finding:

$$\mu_4(\Gamma) \approx \frac{1}{9} \left[ e^{8(1 - \frac{1}{\varepsilon^2 \Gamma})} - 1 \right] \quad . \quad (8)$$

This expression generalizes the result obtained by eqs. 46-47 of Mori and Janssen [16] in the case of a narrow-banded wave train, with less than 5% deviation as compared to their model with a  $(2/3)\alpha^2(\alpha^2 - 1)$  polynomial in the counterpart of eq. (7). In the case of a non-Gaussian sea prior to the shoal, the above equation can be corrected according to eqs. (C1, C7b) of Mendes *et al.* [17]. The excess kurtosis of the experiments in Trulsen *et al.* [19] is well described by eq. (8) (see figure 2). Despite the assumption of Gaussianity prior to the shoal the agreement with observed kurtosis is reasonable, especially in deeper water. Our model rises a little earlier than measured data during the shoaling and later during the de-shoaling, while the trend of the peak in kurtosis to decrease towards deeper waters as well as its magnitude are well estimated. In the comparison, we employed the empirical [18] asymmetry  $\mathfrak{S}(\alpha = 2) = 6/5$ . In the next section we validate this approximation for the ranges

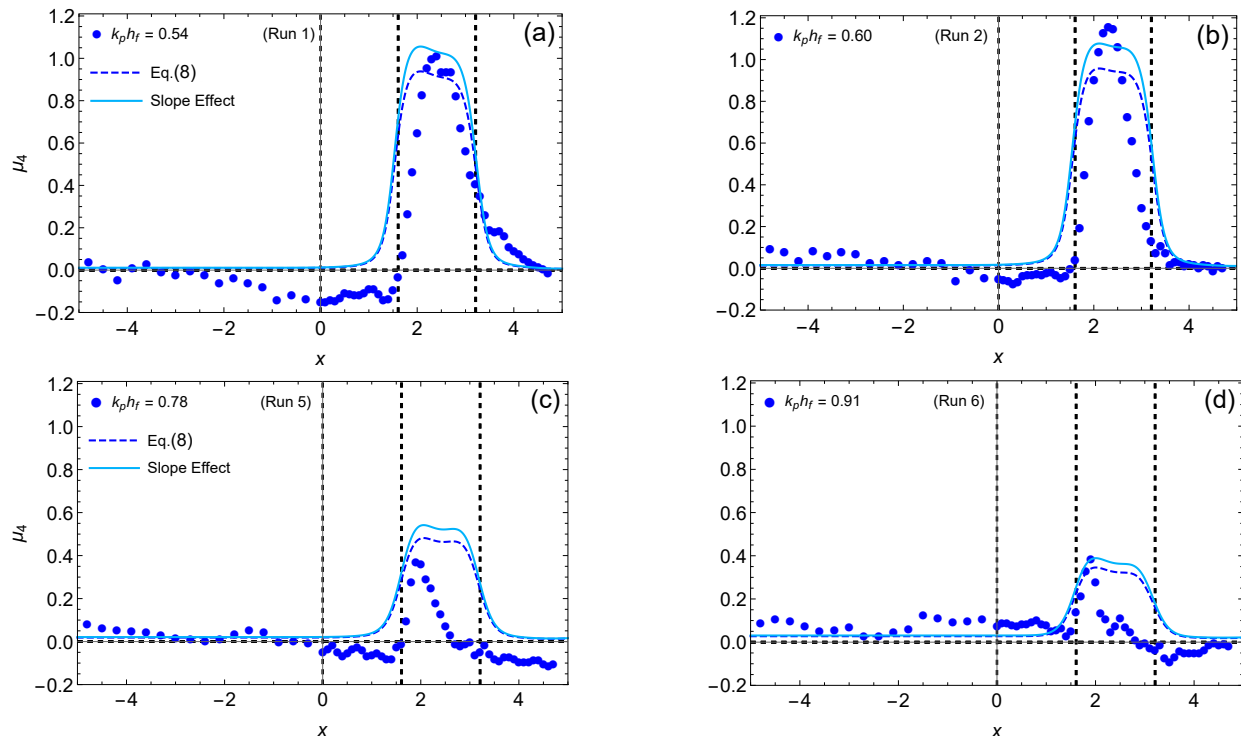


FIG. 2: Kurtosis  $\mu_4$  (dots) of Runs 1, 2, 5, and 6 in Trulsen *et al.* [19] versus the model of eq. (8) (dashed). Dashed vertical lines mark the shoaling and de-shoaling zones (see figure 1). Solid curves include the slope effect [26].

$k_p h \gtrsim \pi/10$ ,  $\nu \lesssim 1/2$  (bandwidth) and  $\varepsilon \ll 1/10$  representative of Trulsen *et al.*'s experiments.

#### IV. VERTICAL ASYMMETRY IN FINITE DEPTH

Eqs. (4) and (8) highlight the influence of the vertical asymmetry on the evolution of rogue wave occurrence and excess kurtosis over a shoal when in intermediate depths. However, the evolution of this asymmetry due to finite depth effects is not well-known, except that is a slowly varying function of the steepness. Following Marthinsen [15] we may consider the skewness to depend solely on depth and steepness  $\mu_3 = \mu_3(\varepsilon, k_p h)$ , and consequently identify  $\mathfrak{S}(\mu_3) = \mathfrak{S}(\varepsilon, k_p h)$  for any  $\alpha$ . The skewness can be approximated as (see eq. 19 of Tayfun [27], with  $\mu$  denoting steepness and  $\lambda_3$  the skewness):

$$\begin{aligned} \mu_3(k_p h > \pi) &\approx 3k_1 \sigma (1 - \nu\sqrt{2} + \nu^2) \\ &\equiv 3k_1 \sigma \cdot \mathfrak{B}(\nu) \approx \frac{\pi}{\sqrt{2}} \varepsilon \mathfrak{B}(\nu) \quad , \quad (9) \end{aligned}$$

where  $H_s = \pi\varepsilon/\sqrt{2}k_p$  and  $k_p$  is the peak wavenumber obtained from the spectral mean wavenumber  $k_1$  through  $k_p \approx (3/4)k_1$  [17]. Figure 3a shows that eq. (9) captures the trend very well in deep water ( $k_p h \geq 5$ ). In fact, in the limit of narrow-banded waves the mean ratio reads  $\langle \mu_3/\varepsilon \rangle \approx 2.6$  for  $k_p h \geq 5$ , being in good agreement with

eq. (9). On the other hand, as the depth decreases to intermediate waters the former ratio significantly increases. To account for this finite depth effect, one must include the sub- and super-harmonic coefficients [12]:

$$\begin{aligned} \tilde{\chi}_0 &= \frac{4 \left( 1 + \frac{2k_p h}{\sinh(2k_p h)} \right) - 2}{\left( 1 + \frac{2k_p h}{\sinh(2k_p h)} \right)^2 \tanh k_p h - 4k_p h} \quad ; \\ \frac{\sqrt{\tilde{\chi}_1}}{2} &= \frac{3 - \tanh^2(k_p h)}{2 \tanh^3(k_p h)} \quad , \quad (10) \end{aligned}$$

with notation  $\tilde{\chi}_i$  from Mendes *et al.* [17]. Combining eq. (9) with eq. 11 of Tayfun and Alkhalidi [12], the finite-depth skewness reads approximately:

$$\mu_3 \approx \frac{\pi\varepsilon}{\sqrt{2}} \mathfrak{B}(\nu) \left( \tilde{\chi}_0 + \frac{\sqrt{\tilde{\chi}_1}}{2} \right) \quad . \quad (11)$$

Although Tayfun and Alkhalidi's model is a good fit for  $k_p h > \pi$ , the sum  $\tilde{\chi}_0 + \sqrt{\tilde{\chi}_1}/2$  stays close to unity for  $k_p h \geq 2$ . Hence, the larger values of the ratio  $\mu_3/\varepsilon$  for shallower water ( $2 \leq k_p h \leq \pi$ ) must stem from a dependence of  $\mathfrak{B}(\nu)$  with depth. We therefore seek a function  $\mathfrak{B}(\nu, k_p h) = 1 - \nu\sqrt{2} + f_{k_p h} \cdot \nu^2$  capable of providing a smooth transition from  $f_{k_p h \sim 3} \approx 3.5$  in shallower depths (see figure 3a) to the deep water value  $f_{k_p h = \infty} \sim 1$  (see eq. (9)). Hence, the vertical asymmetry accounting for

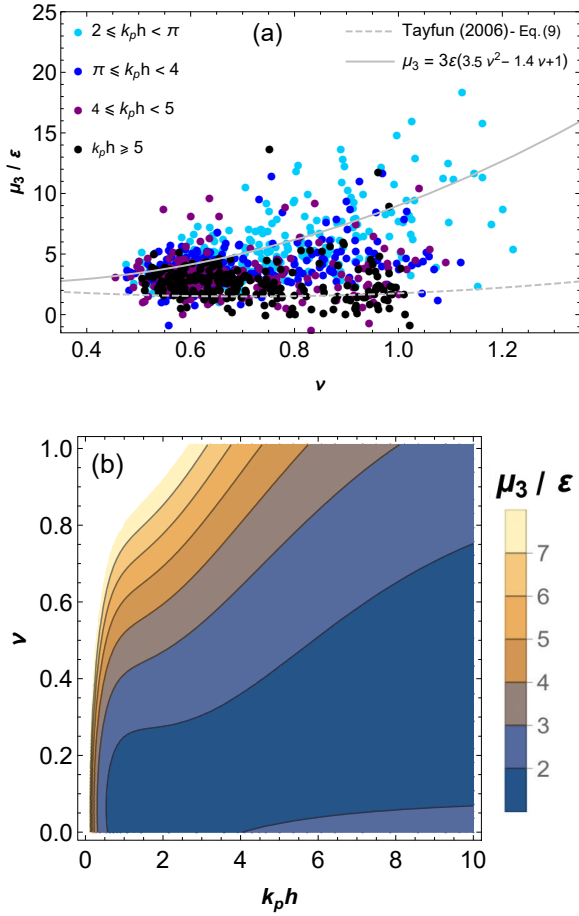


FIG. 3: (a) Ratio of skewness and steepness varying with bandwidth in strongly non-Gaussian ( $\langle \mu_4 \rangle \approx 0.4$ ) North Sea data [18], with numerical polynomial fit  $\mathfrak{B}(\nu) \approx 1 - \nu\sqrt{2} + (7/2)\nu^2$  at  $2 \leq k_p h \leq \pi$ . (b) Contour plot of the same ratio as computed from eq. (11) for the fitted function  $\mathfrak{B}(\nu, k_p h)$  in (a).

depth-induced effects is of the type:

$$\mathfrak{S}(\alpha = 2) \approx \frac{(2 + 6\varepsilon_*)(7 + 3\varepsilon_*)}{6(2 + 3\varepsilon_*)},$$

$$\varepsilon_* \approx \frac{\pi\varepsilon}{3\sqrt{2}} \left[ 1 - \nu\sqrt{2} + f_{k_p h} \cdot \nu^2 \right] \left( \tilde{\chi}_0 + \frac{\sqrt{\tilde{\chi}_1}}{2} \right). \quad (12)$$

Figure 3b provides a contour plot of the empirically fitted model of  $\mathfrak{B}(\nu, k_p h)$ . Here,  $\varepsilon_*$  is the effective steepness and  $f_{k_p h}$  is a function of depth that can be obtained through the constraint of eq (5) applied to eq. (12):

$$\lim_{k_p h \rightarrow 0} \mathfrak{S}(\alpha = 2) \approx \lim_{k_p h \rightarrow 0} \frac{(2 + 6\varepsilon_*)(7 + 3\varepsilon_*)}{6(2 + 3\varepsilon_*)} \leq 2 \quad \therefore$$

$$9\varepsilon_*^2 + 6\varepsilon_* - 5 \leq 0 \quad \therefore \varepsilon_* \leq \frac{\sqrt{6} - 1}{3}. \quad (13)$$

The function  $\mathfrak{B}(\nu, k_p h)$  makes the exceedance probability of rogue waves weakly dependent on the bandwidth. Although the latter is defined in Longuet-Higgins [28] to

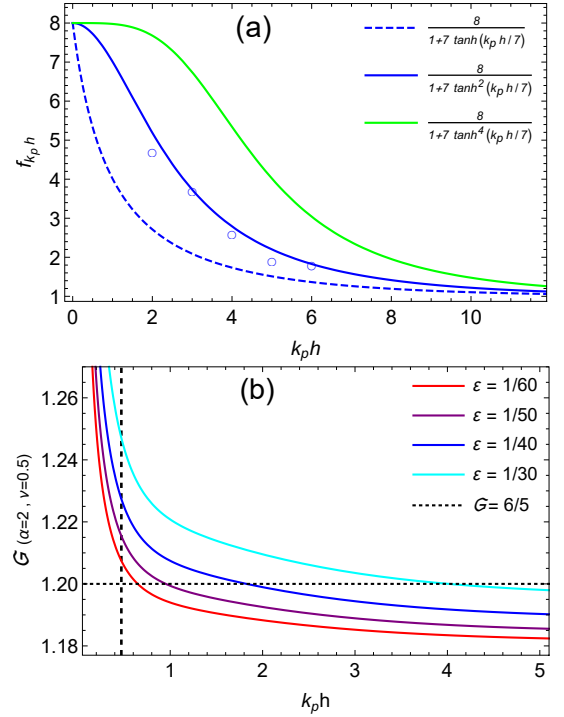


FIG. 4: (a) Finite-depth functions  $f_{k_p h}$  versus data (circles) from figure 3a. (b) Vertical asymmetry of broad-banded rogue waves ( $\nu = 0.5$ ) as a function of water depth for different steepness, with the dotted line depicting the empirical mean value  $\mathfrak{S} = 6/5$  from Mendes *et al.* [17, 18]. Dashed vertical line marks the limit of validity of second-order theory.

have a range  $\nu \in [0, \infty)$ , seas exceeding  $\nu = 1$  account for 3% of observed stormy states in the North Sea [18]. These very extreme sea conditions are typically short-lived and found for instance in hurricanes. Albeit bandwidths much larger than  $\nu = 1$  can increase the vertical asymmetry in about 5-10%, their lifespan makes the weighted exceedance probability of rogue waves over a daily forecast to be slightly deviated ( $\sim 10\%$ ). Accordingly, we may set  $\nu = 1$  as the realistic and effective maximum bandwidth to be considered for estimating the exceedance probability. Hence, in the limit of second-order waves ( $k_p h \rightarrow 1/2$ ) we obtain:

$$\frac{\pi\varepsilon f_{k_p h}}{3\sqrt{2}} \left( \tilde{\chi}_0 + \frac{\sqrt{\tilde{\chi}_1}}{2} \right) < \frac{\sqrt{6} - 1}{3} \quad \therefore f_{k_p h} \lesssim \frac{18\sqrt{2}}{\pi}, \quad (14)$$

valid for  $\nu \leq 1$ . Broad-banded waves have an effective steepness of the order of  $\varepsilon f_{k_p h} \nu^2$ . Since finite-depth effects involve the ratio  $\varepsilon/k_p h$  as it is directly related to  $H_s/h$  we expect  $f_{k_p h} \sim (k_p h)^{-n}$  with  $n \in \mathbb{N}^*$ . In order to fulfill eqs. (13-14), a sigmoid function with continuous derivative providing the best fit for the North Sea data reads (see figure 4a):

$$f_{k_p h} \approx \frac{8}{1 + 7 \tanh^2(k_p h/7)}, \quad \nu \leq 1. \quad (15)$$



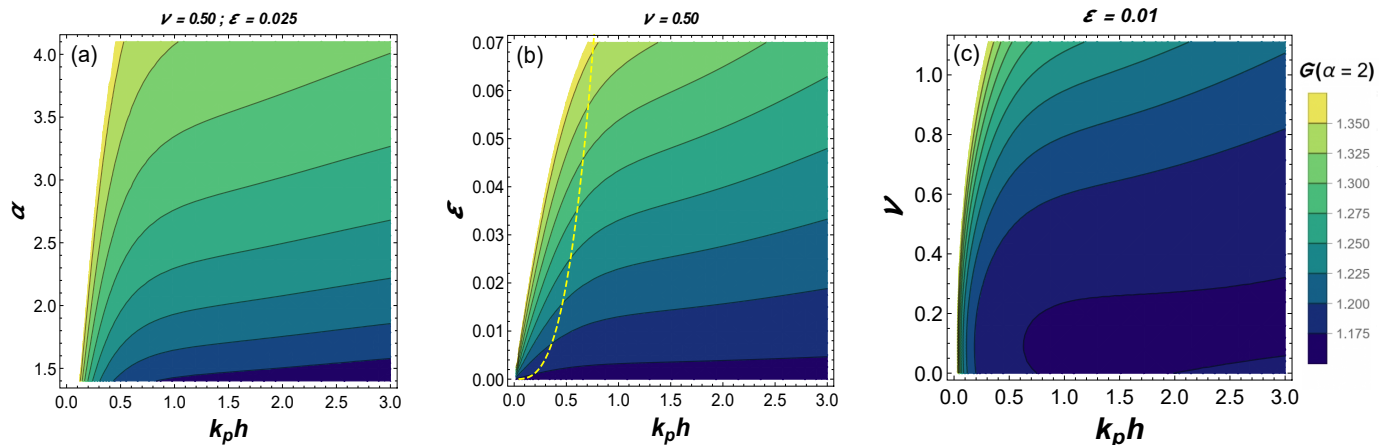


FIG. 5: Vertical asymmetry of large and rogue waves as a function of water depth for different steepness, bandwidth and normalized height. The dashed line in panel b represents the Ursell limit for second-order theory.

Plugging eq. (15) into eq. (12) introduces an approximation for the vertical asymmetry covering the entire range of second-order theory for narrow and broad-banded irregular waves. In fact, figure 4b shows that the vertical asymmetry is almost constant for typical values of steepness ( $\varepsilon \ll 1/10$ ) in intermediate and deep waters ( $k_p h \geq \pi/10$ ). Conversely, sharp increases in the steepness will induce a few percent increase in the vertical asymmetry in the same regimes ( $k_p h \geq \pi/10$ ). The contour plot in figure 5b provides a full description of the variations in asymmetry with depth and steepness. Furthermore, figure 5a shows that in shallow depths the vertical asymmetry strongly depends on  $k_p h$  while in deep water it tends to saturate. Figure 5c also testifies to the role of bandwidth in increasing the asymmetry, albeit sharp changes are restricted to sufficiently broad spectra ( $\nu > 1$ ). Thus, we conclude that unless the steepness in intermediate water is too large ( $\varepsilon > 1/10$ ) or the spectrum very broad ( $\nu > 1/2$ ), sharp variations of the vertical asymmetry occur only in shallow waters ( $k_p h < \pi/10$ ) and otherwise upholds the approximation  $\mathfrak{S} = 6/5$  used above (section III) and Mendes *et al.* [17].

Moreover, the special case of narrow-banded ( $\nu = 0$ ) linear waves ( $\varepsilon \ll 1/10$ ) in deep water leads to  $\varepsilon_* \rightarrow 0$ , thus reaching the asymmetry lower bound  $\mathfrak{S} = 7/6$  for rogue waves. This suggests that in intermediate waters narrowing the bandwidth from  $\nu = 0.3$  to  $\nu = 0$  will have little impact on the amplification of rogue wave statistics due to the negligible change in vertical asymmetry, whereas in shallow water increasing the bandwidth above  $\nu = 0.5$  will be significant. From the point of view of the theory in Mendes *et al.* [17], the asymmetry approximation of eqs. (12,15) explains why narrow-banded models [29] are successful in predicting rogue wave statistics travelling past a step in a broad-banded irregular wave background in intermediate water. Provided there is no wave breaking ( $H_s/h \ll 1$ ), the bandwidth effect will play a role in amplifying statistics in shallower depths because of the contribution of the term  $f_{k_p h} \nu^2$ , as experimentally

demonstrated in Doeleman [30].

## V. UPPER BOUND FOR KURTOSIS

For naval design purposes, the assessment of maximum expected waves over a specific return time is crucial. Typically, ocean structures and vessels must be designed to sustain expected maximum extreme waves over their lifespan [31, 32]. Therefore, we will assess the upper bound for kurtosis over a shoal in the same fashion we obtained eq. (8), but now for the region where there is a balance between the contribution of skewness and kurtosis in the cumulant expansions (atop the shoal). In order to do so, we shall evaluate maxima for the parameters ( $\mathfrak{S}, \Gamma$ ). Possessing an in-depth formula for the vertical asymmetry, we can estimate the upper bound (henceforth denoted by  $\infty$ ) for kurtosis of wave trains of second-order in steepness. Eqs. (12) and (15) provide the upper bound for the vertical asymmetry of rogue waves:  $\mathfrak{S}_\infty(k_p h = \infty) \approx 7/5$  in deep water, and  $\mathfrak{S}_\infty(k_p h = 0) \approx 5/3$  in shallow water. Since the steepness growth due to shoaling is limited to  $\varepsilon \leq 1/7$  by wave breaking, one finds the bound  $\Gamma_\infty - 1 \lesssim 1/12$  due to eq. (3.17) of Mendes *et al.* [17]. Hence, we may approximate:

$$1 - \frac{1}{\mathfrak{S}_\infty^2 \Gamma_\infty} \approx 8(\Gamma_\infty - 1) \quad . \quad (16)$$

Approaching the value  $\Gamma_\infty$  atop the shoal, the contribution of the skewness for the amplification of wave statistics increases as compared to the shoaling zone [33], such that the relationship between kurtosis and skewness leading to eq. (7) is modified and now follows  $\mu_4 \approx \mu_3^2$ . Then, we are able to compute the upper bound for the excess kurtosis with the assumption of a pre-shoal Gaussian statistics (see figure 6):

$$e^{16\alpha^2(\Gamma_\infty - 1)} \approx 1 + \alpha^2 (\alpha^2 - 1) \mu_4 \quad , \quad (17)$$

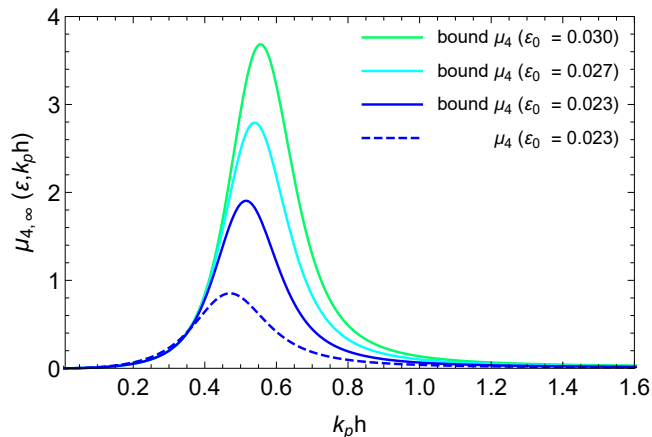


FIG. 6: Upper bound on kurtosis from eq. (18) for  $\nu = 0.5$  and different pre-shoal steepness  $\varepsilon_0$  subject to linear shoaling. The dashed curve represents the computed kurtosis in figure 2a, representative of Run 1 of Trulsen *et al.* [19].

Ergo,

$$\mu_{4, \infty} \approx \frac{1}{12} \left[ e^{64(\Gamma_{\infty}-1)} - 1 \right] \quad , \quad (18)$$

where  $\Gamma_{\infty}$  varies with water depth. According to eq. (18), steep and highly asymmetrical broad-banded waves lead to an upper bound for kurtosis of the order of  $\mu_{4, \infty} \sim 4$ , see figure 6. To give some context, for the special case of a pre-shoal steepness  $\varepsilon = 0.023$  as in Run 1 (dashed blue curve of figure 6) of the experiments of Trulsen *et al.* [19] the observed kurtosis was approximately  $\mu_4 \approx 1$ , whereas our results bound the maximum kurtosis for this experimental set-up to be twice the observed value (solid blue curve of figure 6). We already described that  $\Gamma$  will peak around  $k_p h \approx 0.5$  in Mendes *et al.* [17], and now the excellent agreement with experiments in figure 2 allows us to conclusively assert that the excess kurtosis will also

peak in this region. Furthermore, experimental evidence for the kurtosis reaching a maximum in this region has been recently described in Zhang *et al.* [34].

## VI. CONCLUSIONS

In this work we have extended the framework in Mendes *et al.* [17] to an effective theory for the evolution of excess kurtosis of the surface elevation over a shoal of finite and constant steep slope. We find excellent quantitative agreement during and atop the shoal of experiments in Trulsen *et al.* [19]. Here we have shown that the kurtosis also depends on the inhomogeneities of the energy density over a shoal, whereas the groundwork of Marthinsen [15] computes the excess kurtosis directly from the solution  $\zeta(x, t)$ . On the other hand, a computation of the kurtosis from the probability density of  $\zeta(x, t)$  through the non-homogeneous framework will be pursued in a future work with an analytical non-uniform distribution of random phases.

Furthermore, we have obtained an approximation for the vertical asymmetry in finite depth as a function of both steepness and bandwidth. This approximation recovers the seminal work of Tayfun [27] for the skewness of the surface elevation in narrow-banded deep water waves. Building on this new approximation, we have demonstrated that the vertical asymmetry varies slowly over a shoal in both deep and intermediate waters. Moreover, we were able to compute the maximum possible excess kurtosis driven by shoaling inhomogeneities.

## VII. ACKNOWLEDGMENTS

S.M and J.K. were supported by the Swiss National Science Foundation under grant 200020-175697. We thank Maura Brunetti and Alexis Gomel for fruitful discussions.

- 
- [1] G. Clauss, Dramas of the sea: episodic waves and their impact on offshore structures, *App. Ocean Res.* **24**, 147 (2002).
  - [2] A. Toffoli, T. Waseda, H. Houtani, L. Cavaleri, D. Greaves, and M. Onorato, Rogue waves in opposing currents: an experimental study on deterministic and stochastic wave trains, *Journal of Fluid Mechanics* **769**, 277–297 (2015).
  - [3] S. Haver, A possible freak wave event measured at the draupner jacket january 1 1995, *Proc. Rogue Waves 20-22 October IFREMER* (2004).
  - [4] N. Akhmediev, A. Ankiewicz, and M. Taki, Waves that appear from nowhere and disappear without a trace, *Phys. Lett. A* **373**, 675 (2009).
  - [5] S. Rice, Mathematical analysis of random noise, *Bell Syst. Tech. J.* **24**, 46 (1945).
  - [6] M. Longuet-Higgins, On the statistical distribution of the heights of sea waves, *Journal of Marine Research* **11**, 245 (1952).
  - [7] G. Forristall, On the distributions of wave heights in a storm, *J. Geophys. Res.* **83**, 2353 (1978).
  - [8] M. A. Tayfun, Narrow-band nonlinear sea waves, *J. Geophys. Res.* **85**, 1548 (1980).
  - [9] I. Karpadakis, C. Swan, and M. Christou, Assessment of wave height distributions using an extensive field database, *Coastal Eng.* **157** (2020).
  - [10] I. Teutsch, R. Weisse, J. Moeller, and O. Krueger, A statistical analysis of rogue waves in the southern north sea, *Natural Hazards and Earth System Sciences* **20**, 2665

- (2020).
- [11] M. Longuet-Higgins, The effect of non-linearities on statistical distributions in the theory of sea waves, *J. Fluid Mech.* **17**, 459 (1963).
  - [12] M. A. Tayfun and M. A. Alkhalidi, Distribution of sea-surface elevations in intermediate and shallow water depths, *Coastal Eng.* **157** (2020).
  - [13] E. M. Bitner, Non-linear effects of the statistical model of shallow-water wind waves, *Applied Ocean Research* **2**, 63 (1980).
  - [14] M. Tayfun, Distribution of large wave heights, *J. Waterway, Port, Coastal Ocean Eng.* **116**, 686 (1990).
  - [15] T. Marthinsen, On the statistics of irregular second-order waves, Report No. RMS-11 (1992).
  - [16] N. Mori and P. Janssen, On kurtosis and occurrence probability of freak waves, *J. Phys. Oceanogr.* **36**, 1471 (2006).
  - [17] S. Mendes, A. Scotti, M. Brunetti, and J. Kasparian, Non-homogeneous model of rogue wave probability evolution over a shoal, *J. Fluid Mech.* **939**, A25 (2022).
  - [18] S. Mendes, A. Scotti, and P. Stansell, On the physical constraints for the exceeding probability of deep water rogue waves, *Appl. Ocean Res.* **108**, 102402 (2021).
  - [19] K. Trulsen, A. Raustøl, S. Jorde, and L. Rye, Extreme wave statistics of long-crested irregular waves over a shoal, *J. Fluid Mech.* **882** (2020).
  - [20] O. Kimmoun, H.-C. Hsu, N. Hoffmann, and A. Chabchoub, Experiments on uni-directional and nonlinear wave group shoaling, *Ocean Dynamics* (2021).
  - [21] B. K. Glukhovskiy, Investigation of sea wind waves (in russian), *Gidrometeoizdat, Leningrad*, , 283 (1966).
  - [22] I. Karpadakis, C. Swan, and M. Christou, A new wave height distribution for intermediate and shallow water depths, *Coastal Engineering* **175**, 104130 (2022).
  - [23] N. Mori and T. Yasuda, A weakly non-gaussian model of wave height distribution random wave train, *Ocean Eng.* **29**, 1219–1231 (2002).
  - [24] S. Mendes, On the statistics of oceanic rogue waves in finite depth: Exceeding probabilities, physical constraints and extreme value theory, UNC Chapel Hill PhD Thesis (2020).
  - [25] N. Mori and N. Kobayashi, Nonlinear distribution of neashore free surface and velocity, in *Coastal Engineering 1998* (1998) pp. 189–202.
  - [26] S. Mendes and J. Kasparian, Saturation of rogue wave amplification over steep shoals, *Phys. Rev. E* **106**, 065101 (2022).
  - [27] M. Tayfun, Statistics of nonlinear wave crests and groups, *Ocean Eng.* **33**, 1589 (2006).
  - [28] M. S. Longuet-Higgins, On the joint distribution of the periods and amplitudes of sea waves, *J. Geophys. Res.* **80**, 2688 (1975).
  - [29] Y. Li, S. Draycott, Y. Zheng, Z. Lin, T. Adcock, and T. Van Den Bremer, Why rogue waves occur atop abrupt depth transitions, *Journal of Fluid Mechanics* **919**, R5 (2021).
  - [30] M. W. Doeleman, Rogue waves in the dutch north sea, Master’s thesis, TU Delft (2021).
  - [31] L. E. Borgman, Probabilities for highest wave in hurricane, *Journal of the Waterways, Harbors and Coastal Engineering Division* **99**, 185 (1973).
  - [32] L. R. Muir and A. El-Shaarawi, On the calculation of extreme wave heights: a review, *Ocean Engineering* **13**, 93 (1986).
  - [33] Y.-X. Ma, X.-Z. Ma, and G.-H. Dong, Variations of statistics for random waves propagating over a bar, *Journal of Marine Science and Technology (Taiwan)* **23**, 864 (2015).
  - [34] J. Zhang, Y. Ma, T. Tan, G. Dong, and M. Benoit, Enhanced extreme wave statistics of irregular waves due to accelerating following current over a submerged bar, *Preprint* submitted to *J. Fluid Mech* (2023).